

Oscillatory dephasing in the presence of inhomogeneous broadening

P. Martin, J. P. Lavoine, A. J. Boeglin, and A. A. Villaeys

*Institut de Physique et Chimie des Matériaux de Strasbourg, Groupe d'Optique Nonlinéaire et d'Optoélectronique,
23 rue du Loess, 67037 Strasbourg-Cedex, France*

(Received 4 June 1996; revised manuscript received 2 August 1996)

Oscillatory dephasing is a characteristic signature of non-Markovian relaxation phenomena. From its analysis one can obtain valuable information about the dynamics of the surroundings of a given system. In this paper we calculate the transient four-wave mixing signal in the short pulse limit from two-level systems coupled to a bath of harmonic oscillators for arbitrary coupling strengths and in the presence of inhomogeneous broadening. The strong and weak coupling cases having already been analyzed, we focus on the study of the intermediate case where oscillatory dephasing is observed. We specifically show that even in the presence of inhomogeneous broadening, information about the surroundings can still be extracted in the intermediate coupling regime. The formation and the evolution of the photon echo in such experiments are also analyzed. [S0163-1829(96)05043-6]

I. INTRODUCTION

The last few years have seen an intense activity in the study of optical line shapes of molecular systems in condensed phases. Special attention was paid to the dynamics of relaxation of vibronic states in complex molecules.¹ For such systems, inhomogeneous broadening is often present so that linear optical experiments are usually poor tools to extract dynamical or structural information from these systems. This broadening results mainly from variations of the local environment of the molecules under investigation, as is usually the case in systems where long range order is absent. However, numerous nonlinear optical techniques, such as hole burning experiments,^{2,3} quantum beat spectroscopy,⁴⁻⁶ or transient four-wave mixing (TFWM),^{7,8} are presently available to extract information even if inhomogeneous broadening is present. For example, in the well known classical photon echo experiments,⁹⁻¹¹ three matter-field interactions give rise to an echo signal due to the presence of an inhomogeneously broadened system. This echo is then time integrated by a detector with a long time response and the integrated intensity gives us information about the dephasing dynamics. Theoretically, it is generally assumed that the relaxation processes of the media under study can be described using two broadening mechanisms: inhomogeneous broadening and homogeneous broadening. The latter is usually described by using time independent constants, or, in other words, it is assumed that the relaxation shows a conventional Markovian exponential decay. In this sense, the works about the dynamical effects in spectral hole burning¹² or, more recently, the experimental TFWM studies of dephasing dynamics of vibronic states,¹³ keep the basic concept of time independent relaxation constants.

With the recent progress in time resolved spectroscopy, laser pulses in the femtosecond time domain can be used to probe ultrafast dynamical processes. From a theoretical point of view, the relaxation on this ultrashort time scale cannot be simply described by the time independent homogeneous constants T_1 for the relaxation of populations and T_2 for the loss of coherences. Non-Markovian behavior due to memory ef-

fects should be taken into account. As Aihara¹⁴ has shown for a TFWM experiment, in the case of strong coupling between a two-level system and its surroundings, these memory effects lead to a photon echo phenomenon. This echo differs in nature from the former due to the collective response of an inhomogeneously broadened set of systems. In fact, on an ultrashort time scale, different physical phenomena may contribute to the relaxation mechanisms and, as was mentioned by Kayanuma,¹⁵ the homogeneous phase relaxation should not be confused with the phase relaxation due to the inhomogeneous distribution of energy. Hence, for short times, it is crucial to take into account the multiple time scale nature of the dynamics of the surroundings to suitably describe the relaxation.

This was done both experimentally and theoretically, using a stochastic model, by Saikan *et al.*^{16,17} They studied the dephasing dynamics in iron free myoglobin in two limiting cases of slow and fast motion of the surroundings in the presence of inhomogeneous broadening. They recovered the predictions given by Yan and Mukamel¹⁸ with the Brownian oscillator model.

However, these models are stochastic in nature.¹⁹ They have been widely used to describe the solvent effects on electronic dephasing for molecules in solution.²⁰⁻²³ They consider that the surroundings of the studied material can be modeled by a frequency modulation of the material levels. This modulation is treated as a stationary random process so that the nonequilibrium motion of the surroundings of the system under optical excitation cannot be described by this approach.

An alternate way consists of modeling the surroundings microscopically.²⁴ This approach allowed Aihara^{25,26} to point out, in the absence of an inhomogeneous contribution, three typical kinds of decay according to the values of the TLS-environment interaction strength. The two preceding limiting cases of fast and slow modulations have been studied. They correspond, respectively, to the Markovian regime and to a situation where a photon echo, due to strong memory effects, appears. The third kind of decay corresponds to the intermediate regime, where the observation time scale is of the same

order as the correlation time of the system-environment interaction. In this case, the non-Markovian relaxation is characterized both by a nonexponential decay and oscillatory dephasing. This is not described by the stochastic approaches. In addition, the situation of intermediate coupling strength is probably more realistic than the strong or weak limits usually considered in theoretical treatments. On the other hand, the samples tested in real experiments generally show large inhomogeneous broadening. Therefore it is of practical importance to find out how inhomogeneous broadening affects oscillatory dephasing and whether information about the surroundings can still be extracted in such experiments. This is the goal of this paper.

The paper is organized as follows. In Sec. II we present the theoretical model. Section III is devoted to the simulations and discussion. We first recover the two limiting cases of fast and slow modulation^{16,18} with our theoretical model. Then, we analyze the effect of inhomogeneous broadening in the intermediate regime of modulation. A simulation of the temporal intensity is presented at the end of the paper in order to clearly distinguish the different contributions in the TFWM signal. In the final section we briefly state our conclusions.

II. FORMALISM

In this work we consider a statistical ensemble of two-level systems (TLS), in interaction with a thermal bath. Each of these TLS interacts with its local surroundings, which are described in a microscopic way as a set of harmonic oscillators. This model applies to various kinds of physical situations, particularly localized electron-phonon systems.²⁷⁻³²

The Hamiltonian for a given TLS is expressed as

$$H_m = H_g |g\rangle\langle g| + H_e |e\rangle\langle e|, \quad (2.1)$$

with

$$H_g = \sum_k \hbar \omega_k (b_k^\dagger b_k + \frac{1}{2}), \quad (2.2)$$

$$H_e = H_g + \hbar \omega_{eg} + V, \quad (2.3)$$

where $|g\rangle$, $|e\rangle$ are the electronic eigenstates of the TLS, and where b_k (b_k^\dagger) is the annihilation (creation) operator for the k th phonon mode with frequency ω_k . H_g and H_e are thus operators in the reservoir variables. They describe the bath Hamiltonian in the ground and excited electronic states, re-

spectively. The electron-phonon interaction Hamiltonian V is given in terms of linear and quadratic parts,³³

$$V = \sum_k h_L \omega_k (b_k + b_k^\dagger) + \frac{1}{2} \sum_k \sum_q h_Q \sqrt{\omega_k \omega_q} (b_k + b_k^\dagger) (b_q + b_q^\dagger), \quad (2.4)$$

where h_L and h_Q are the linear and quadratic dimensionless interaction constants taken to be independent of the bath modes.

This system interacts with a coherent field, treated classically here, which induces transitions between the two electronic levels. In the dipole approximation, the radiation-matter interaction Hamiltonian is given by

$$H_1(\mathbf{r}, t) = -\boldsymbol{\mu} \cdot \mathbf{E}(\mathbf{r}, t), \quad (2.5)$$

where $\boldsymbol{\mu}$ is the dipole-moment operator and $\mathbf{E}(\mathbf{r}, t)$ is the electric field:

$$\mathbf{E}(\mathbf{r}, t) = \sum_\alpha \{ \mathcal{E}_\alpha(t) \exp[i(\omega t - \mathbf{k}_\alpha \cdot \mathbf{r})] + \text{c.c.} \}. \quad (2.6)$$

In the following, we shall assume that the matrix elements of the dipole operator are real and independent of the bath variables and, since this is of no consequence in the study performed here, the electric field and the transition dipole moments are parallel.

As in many quantum statistical problems, the dynamical state of the system is best described with the help of the density operator $\rho(t)$, which satisfies the well known Liouville equation of motion

$$\frac{d\rho}{dt} = -\frac{i}{\hbar} [H_m + H_1(\mathbf{r}, t), \rho]. \quad (2.7)$$

We further assume that, at the initial time, the TLS and the bath are uncorrelated, namely, $\rho(-\infty) = |g\rangle\langle g| \rho_R$, where $\rho_R = \exp(-\beta H_g) / \text{Tr}_{\text{bath}}[\exp(-\beta H_g)]$ represents the density operator of the bath at thermal equilibrium. An approximate solution of Eq. (2.7) for the density operator is obtained by performing a perturbative expansion up to the third order in the matter-field interaction. Thus, the third order off-diagonal elements of the reduced density operator, $\sigma_{eg}^{(3)}(t) = \text{Tr}_{\text{bath}}[\rho_{eg}^{(3)}(t)]$, for the collection of TLS, take the following form:

$$\begin{aligned} \sigma_{eg}^{(3)}(\mathbf{r}, t) = & \frac{-i\mu_2^3}{\hbar^3} \int_0^\infty d\omega_{eg} g(\omega_{eg}) \int_{-\infty}^t dt_1 \int_{-\infty}^{t_1} dt_2 \int_{-\infty}^{t_2} dt_3 E(\mathbf{r}, t_1) E(\mathbf{r}, t_2) E(\mathbf{r}, t_3) \\ & \times \text{Tr}_{\text{bath}} \left\{ \left[\exp\left(-\frac{i}{\hbar} H_m^g(t-t_1)\right) \exp\left(-\frac{i}{\hbar} H_m^e(t_1-t_3)\right) \rho_R \exp\left(\frac{i}{\hbar} H_m^g(t_2-t_3)\right) \exp\left(\frac{i}{\hbar} H_m^e(t-t_2)\right) \right] \right. \\ & + \left[\exp\left(-\frac{i}{\hbar} H_m^g(t-t_1)\right) \exp\left(-\frac{i}{\hbar} H_m^e(t_1-t_2)\right) \exp\left(-\frac{i}{\hbar} H_m^g(t_2-t_3)\right) \rho_R \exp\left(\frac{i}{\hbar} H_m^e(t-t_3)\right) \right] \\ & + \left[\exp\left(-\frac{i}{\hbar} H_m^g(t-t_2)\right) \exp\left(-\frac{i}{\hbar} H_m^e(t_2-t_3)\right) \rho_R \exp\left(\frac{i}{\hbar} H_m^g(t_1-t_3)\right) \exp\left(\frac{i}{\hbar} H_m^e(t-t_1)\right) \right] \\ & \left. + \left[\exp\left(-\frac{i}{\hbar} H_m^g(t-t_3)\right) \rho_R \exp\left(\frac{i}{\hbar} H_m^e(t_2-t_3)\right) \exp\left(\frac{i}{\hbar} H_m^g(t_1-t_2)\right) \exp\left(\frac{i}{\hbar} H_m^e(t-t_1)\right) \right] \right\}, \quad (2.8) \end{aligned}$$

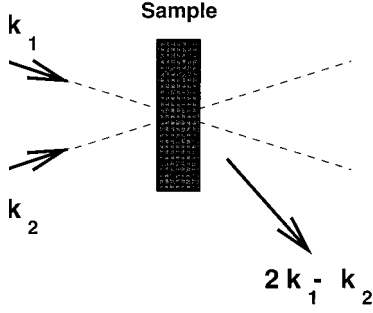


FIG. 1. Experimental configuration of a TFWM experiment.

where $g(\omega_{eg})$ is an inhomogeneous distribution of the transition energies ω_{eg} of the TLS taking into account the variations in their local environments.

It should be noted that, at this stage, no assumption regarding the explicit form of the fields is made. Hence, Eq. (2.8) can be applied to any nonlinear optical phenomena involving three matter field interactions. However, in the following, we will restrict ourselves to the particular case of photon echo experiments (see Fig. 1), where two short laser pulses $E_1(\mathbf{r}, t - \tau)$ and $E_2(\mathbf{r}, t)$ with the same frequency, but with different wave vectors, are sequentially applied to the system with a time interval τ . The expression of the third order polarization, $\mathcal{P}^{(3)}$, responsible for the echo signal emitted in the $2\mathbf{k}_1 - \mathbf{k}_2$ direction, reduces to the contribution

$$\mathcal{P}^{(3)} = \text{Tr}_{\text{material}}[\boldsymbol{\mu}\sigma^{(3)}] = \boldsymbol{\mu}\sigma_{eg}^{(3)} + \text{c.c.} \quad (2.9)$$

$$= \mathcal{P}^{(3)}(t) \exp[i(\omega t - (2\mathbf{k}_1 - \mathbf{k}_2) \cdot \mathbf{r})] + \text{c.c.} \quad (2.10)$$

Given the femtosecond time scale for the pulse widths, we apply the rotating wave approximation and assume that the time variations of the field envelopes $\mathcal{E}_1(t)$ and $\mathcal{E}_2(t)$ are fast compared to all other characteristic time scales of the dynamics of the system. We can apply the approximation of δ pulses and perform all the temporal integrations in relation (2.8) to calculate the macroscopic polarization. $\mathcal{P}^{(3)}(t)$, aside from unimportant multiplicative factors, takes the form

$$\begin{aligned} \mathcal{P}^{(3)}(t, \tau) &= \mu^4 \int_{-\infty}^{\infty} d\Delta g(\Delta) \exp[i\Delta(t - 2\tau)] \\ &\times \exp[Q(-\tau, \tau, t - \tau)/\hbar^2], \end{aligned} \quad (2.11)$$

where the quantity Δ is equal to $\omega - \omega_{eg} - \langle V \rangle / \hbar$ and $Q(-\tau, \tau, t - \tau)$ is a complex function of its time arguments. For the evaluation of Q , the readers should refer to Ref. 33, where the authors have used the cumulant expansion method up to second order¹⁸ to study the effects of the non-Markovian oscillations on quantum beats.

The intensity and the integrated intensity of radiation emitted in the direction $2\mathbf{k}_1 - \mathbf{k}_2$ are then given by

$$I(\tau, t) = |\mathcal{P}^{(3)}(\tau, t)|^2, \quad (2.12)$$

$$I(\tau) = \int_{-\infty}^{\infty} I(\tau, t) dt. \quad (2.13)$$

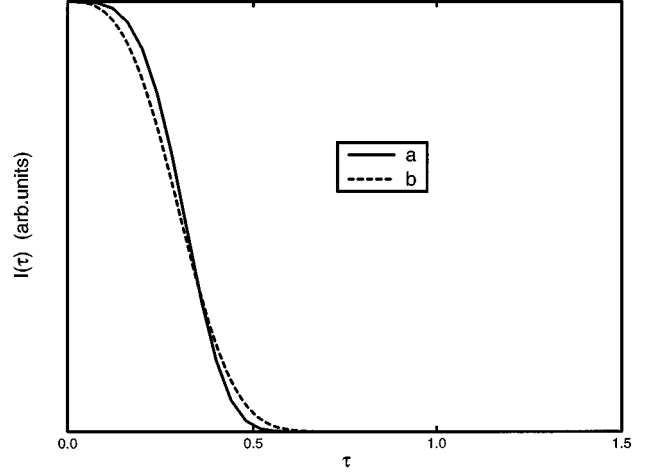


FIG. 2. Time-integrated intensity as a function of the pulse delay τ . The time axis is normalized by the phonon oscillation ω_p . $\beta = 1$, $\gamma_p = 0.4$, and $\mu = 1$, $h_L = 5$, $h_Q = 0.8$. Curve *a* corresponds to $\gamma_{ei} = \infty$. Curve *b* represents the fitting function $\exp(-a\tau^3)$.

In our calculation we have assumed that the inhomogeneous broadening stems from a Gaussian distribution of the transition frequencies with a maximum centered at the field frequency and with the width γ_{ei} . The inhomogeneous contribution, as is usually the case, is considered as a static property of the sample under study. It is taken into account, in an *ad hoc* way, by the distribution of transition energies. In addition, the bath is responsible for all the dynamical effects on the experimental time scale. It is assumed to keep the same physical characteristics for each TLS and, therefore, is independent of the inhomogeneous distribution. $I(\tau, t)$ thus becomes

$$\begin{aligned} I(\tau, t) &= \mu^4 \exp[-(t - 2\tau)^2 \gamma_{ei}^2] \\ &\times \exp[2\text{Re}(Q(-\tau, \tau, t - \tau)/\hbar^2)], \end{aligned} \quad (2.14)$$

where Re denotes the real part. In the case of an infinite inhomogeneous broadening, Eq. (2.7) can be integrated analytically, yielding

$$I(\tau) = \mu^4 \exp[2\text{Re}(Q(-\tau, \tau, t - \tau)/\hbar^2)]. \quad (2.15)$$

III. SIMULATIONS

In all the simulations presented in this work, we have assumed that the phonon density of states has a Gaussian profile with the maximum at ω_p and with the width γ_p .²⁵ The integration which appears in relations (2.14) and (2.15) has been achieved numerically. Moreover, since we restrict ourselves to a qualitative discussion, all the intensities have been normalized to unity.

We first test our theoretical model by showing that we recover the strong and weak coupling situations, already described in the literature. These two limiting cases are illustrated by Figs. 2 and 3. These figures differ in the value of the interaction constants h_L and h_Q but, otherwise, all the parameters are identical and correspond to the numerical simulations in Aihara's work.²⁵

The strong coupling limit corresponds to Fig. 2. As can be

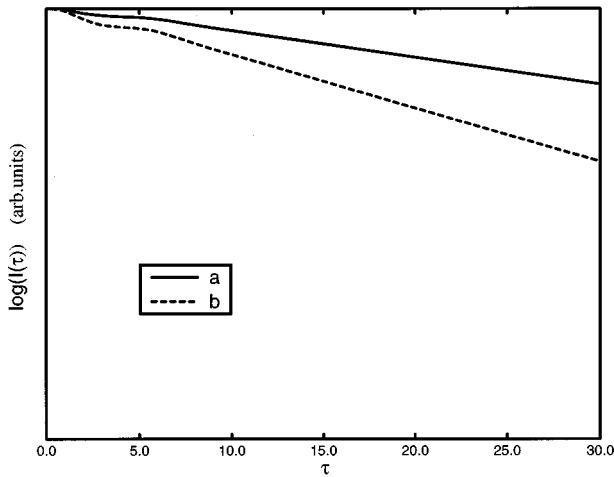


FIG. 3. Time-integrated intensity as a function of the pulse delay τ . $h_L=0.05$, $h_Q=0.008$. Curve *a* corresponds to the case without inhomogeneous broadening ($\gamma_{ei}=0$), curve *b* with an infinite inhomogeneous broadening ($\gamma_{ei}=\infty$), otherwise all constants are identical to the ones taken in Fig. 2.

seen in curve *a*, the signal does not exhibit an exponential decay as is the case in the conventional photon echo where Markovian dephasing occurs. Nevertheless, curve *b*, representing $\exp(-a\tau^3)$, approximates our theoretical results closely by a proper choice of the parameter *a*. This result is coherent with the theoretical work of Yan and Mukamel,¹⁸ which has already predicted such a dependence in the framework of the Brownian oscillator model and the experimental work of Saikan *et al.*¹⁶

To complete the test of our theoretical model, we have represented in Fig. 3 a situation corresponding to the opposite limit of weak coupling. We recover the well known exponential decay characteristic of the Markovian regime and by comparing the homogeneous [Fig. 3 curve *a*] and the inhomogeneous [Fig. 3 curve *b*] cases we also recover the well known ratio of two between the decay rates.³⁴ From a

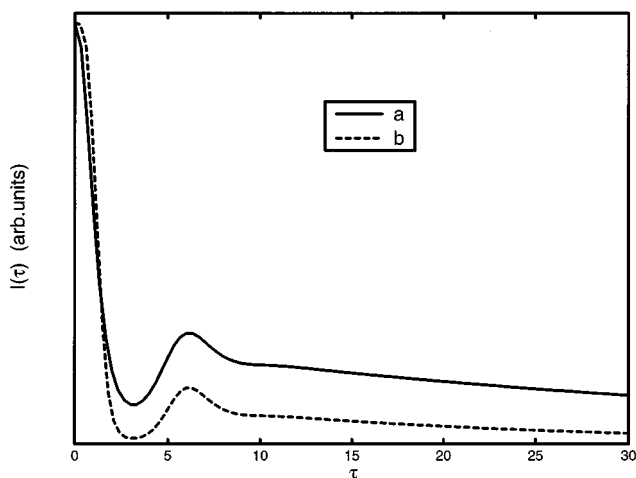


FIG. 4. Time-integrated intensity as a function of the pulse delay τ . The constants are identical to the ones taken in Fig. 3 except that here $h_L=0.4$, $h_Q=0.066$, and $\gamma_{ei}=0$ for curve *a* and $\gamma_{ei}=\infty$ for curve *b*.

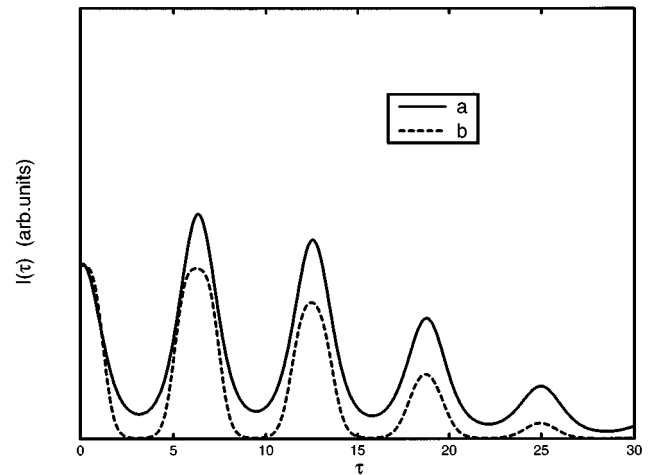


FIG. 5. Time-integrated intensity as a function of the pulse delay τ . The constants are identical to the ones taken in Fig. 4, except that here $\gamma_p=0.05$ and $\gamma_{ei}=0$ for curve *a* and $\gamma_{ei}=\infty$ for curve *b*.

theoretical point of view, it should be noted that these two limiting situations are both well described in the framework of the stochastic model and we need not resort especially to a microscopic description of the relaxation mechanism. This can be explained by the fact that, in the two preceding cases, the bath induced modulation can be considered either as static or as ultrafast in comparison with the time scale of the signal decay for the microscopic characteristics of the bath to play a significant role in the system's dynamics.

The simulations in Figs. 4 and 5 correspond to the situation of intermediate values of the system-bath coupling parameters. The labels *a* and *b* on these curves correspond to a situation without and with inhomogeneous broadening, respectively. In Fig. 4, the numerical parameters are chosen to lead to only one well resolved non-Markovian oscillation in the integrated signal in order to clearly distinguish the

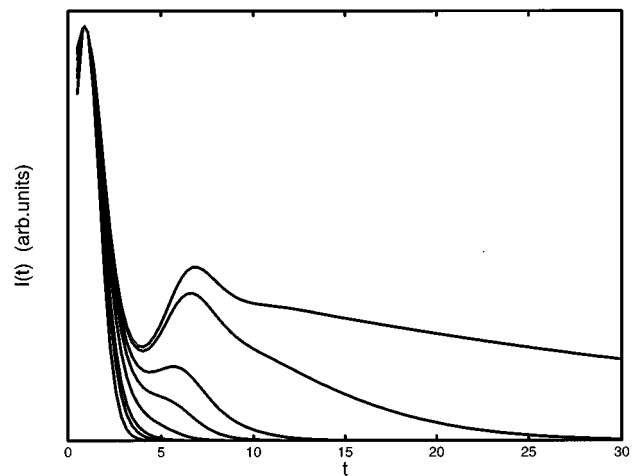


FIG. 6. Nonintegrated intensity as a function of the time t . The time delay is $\tau=0.5$. The constants are identical to the ones taken in Fig. 4, except that here the inhomogeneous broadening is finite and $\gamma_{ei}=0.01, 0.1, 0.25, 0.35, 0.5, 0.7, 0.8,$ and 1 for the curves taken from the top to the bottom.

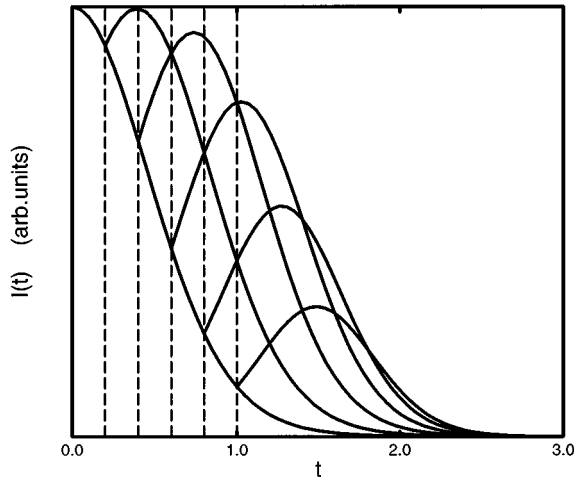


FIG. 7. Nonintegrated intensity as a function of the time t for time delays $\tau=0.0, 0.2, 0.4, 0.6, 0.8, 1.0$, indicated by vertical dashed lines. $h_L=1$, $h_Q=0.158$, and $\gamma_{ei}=0.5$, the other constants being identical to those in Fig. 6.

non-Markovian part and the Markovian part of the signal. Comparing curves a to b , we immediately observe that the signal has a weaker intensity in the presence of an infinite inhomogeneous broadening. This fact is not surprising since this corresponds to a system with a dilute resonance frequency energy distribution. However, we notice that the presence of an inhomogeneous broadening does not affect drastically the overall profile of the decay. For short time delays, the non-Markovian oscillation is still well resolved. Furthermore, for short delays, the competition between the rephasing process at time 2τ after the first applied pulse, due to the inhomogeneous contribution, and the non-Markovian oscillatory dephasing processes accentuates the slope of the intensity decay, and leads to a better contrast for the non-Markovian oscillation. This tendency is clearly confirmed in Fig. 5, where the non-Markovian behavior leads to stronger oscillations. For that, we have used a sharper phonon density so as to increase the oscillatory dephasing. In curve b , we observe a faster damping of the oscillations. The non-Markovian oscillations not only persist on the whole of the signal, but are clearly better resolved than they are in curve a , where the inhomogeneous contribution is absent. Therefore, and this is the main result of this work, in the intermediate case, the presence of an inhomogeneous broadening does not affect drastically the behavior of the signal detected as a function of the time delay between pulses. In particular, we notice that the frequency of the oscillation remains constant. Only the contrast is modified. This point is important because it means that experimental results, obtained in TFWM experiments, can still be used to analyze memory effects even in the presence of inhomogeneous broadening.

In order to clearly distinguish the different contributions our model can take into account in the signal decay and to analyze how the rephasing processes due to inhomogeneous broadening can act, we have studied the nonintegrated intensity. Given femtosecond light pulse widths, this nonintegrated intensity is obviously not accessible experimentally.

Nevertheless, it will allow us to confirm the usual effects of inhomogeneous broadening on the coherence. To this end,

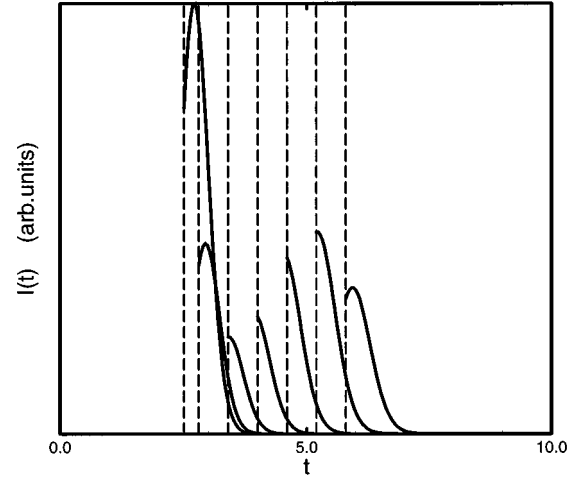


FIG. 8. Nonintegrated intensity as a function of the time t for time delays $\tau=2.5, 2.8, 3.4, 4.0, 4.6, 5.2, 5.8$, indicated by vertical dashed lines. $h_L=1$, $h_Q=0.158$, and $\gamma_{ei}=0.5$, the other constants being identical to those in Fig. 6.

we have represented the nonintegrated intensity for a fixed short time delay and for increasing values of the inhomogeneous width in Fig. 6. Starting from a well resolved non-Markovian oscillation, it becomes less and less pronounced as the width increases. For a sufficiently large value it disappears totally. As expected, the coherence is totally suppressed for a sufficiently large inhomogeneous width.

Moreover, our model enables us to also analyze the evolution and the formation of the echo. This is of interest because in the case of strong coupling and for a short delay, an echo due to memory effect occurs. In addition, an echo due to the inhomogeneous contribution should be observable in the nonintegrated intensity. Increasing the time delay between the two applied pulses, we show the formation and the temporal evolution of these different echoes in the simulations Fig. 7 to Fig. 10. Here, we have considered a finite inhomogeneous broadening, to clearly distinguish the different contributions. The vertical dashed lines show the arrival time of the second pulse. Moreover, we should keep in mind that the intensity decreases when the delay time increases but, for clarity, all the curves, which correspond to the lowest delay time in each graph, are normalized to unity. Starting with time delays shorter than the correlation time of the system-bath interaction, we obtain, in Fig. 7, the echo phenomenon already mentioned and due to memory effects. On these short time scales, inhomogeneous broadening is not in competition with the precedent echo because we have considered a finite width. Notice that larger widths may act on the same short time scale. Increasing τ , we observe in Fig. 8 the oscillatory behavior of the signal emitted after the second laser pulse and characteristic of the memory effects. It is responsible for the oscillatory behavior in the integrated signal. In Fig. 9, the time delay has become of the same order as the correlation time of the system-bath interaction and we can observe the non-Markovian oscillation reflecting the bath dynamics. Due to the particular choice of its width, the inhomogeneous broadening contributes on this time scale. It can be observed, in the same figure (Fig. 9), that an echo phenomenon due to inhomogeneous broadening appears on

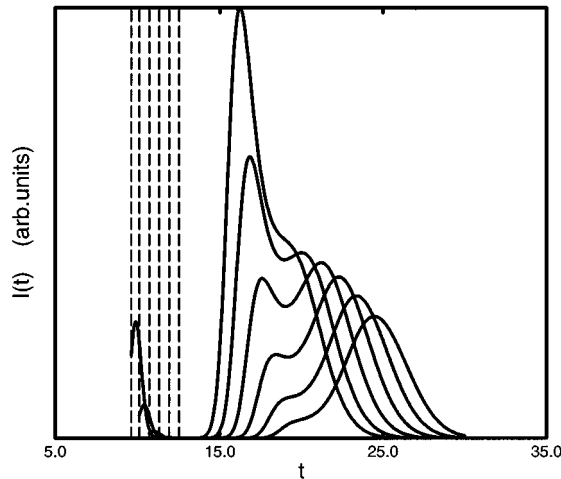


FIG. 9. Nonintegrated intensity as a function of the time t for time delays $\tau=9.6, 10.1, 10.7, 11.3, 11.9, 12.5$, indicated by vertical dashed lines. $h_L=1$, $h_Q=0.158$, and $\gamma_{ei}=0.5$, the other constants being identical to those in Fig. 6.

the left and coexists with the oscillation precedently described. It becomes well resolved in Fig. 10. This latter corresponds to the Markovian regime and the decay of the echo follows a conventional exponential decay.

IV. CONCLUSION

In this paper, we have analyzed the transient nonlinear optical response of an inhomogeneously broadened set of two-level systems. We have used a microscopic description to model the interaction between the TLS and their environments, which have been described as a set of harmonic oscillators. This model can be applied to various kinds of materials including localized electron-phonon systems. Our model enables us to consider arbitrary coupling strengths between the TLS and the bath. We have recovered the well known situations corresponding to the strong and weak coupling limits that have already been analyzed with the help of stochastic models. Here, we have considered the case of intermediate couplings and have studied the influence of inho-

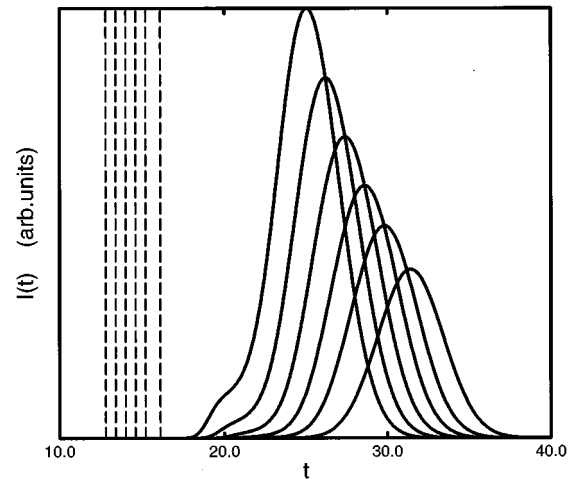


FIG. 10. Nonintegrated intensity as a function of the time t for time delays $\tau=12.8, 13.4, 14.0, 14.6, 15.2, 16.1$, indicated by vertical dashed lines. $h_L=1$, $h_Q=0.158$, and $\gamma_{ei}=0.5$, the other constants being identical to those in Fig. 6.

mogeneous broadening on the photon echo signal. It has been found that non-Markovian oscillations, reflecting the memory effects, are not drastically affected by the rephasing processes due to a strong inhomogeneous broadening. Moreover, for a situation which leads to strong oscillations in the signal decay, a better contrast in the oscillatory behavior is obtained. This result shows that for intermediate TLS-bath coupling strengths, information on the bath can still be extracted in such experiments. The frequency of the oscillations is not modified by the presence of inhomogeneous broadening. This latter acts only on the contrast of the signal. In addition, a study of the nonintegrated intensity enabled us to show the different physical contributions to the dephasing processes our model can take into account. The formation and the evolution of the echoes due to memory effects, on one hand, and inhomogeneous broadening, on the other hand, have been studied. They enable us to show how the different physical phenomena can act on different time scales.

¹S. Mukamel, *Principle of Nonlinear Spectroscopy* (Oxford University Press, New York, 1995).

²D. Haarer and R. Silbey, *Phys. Today* **43** (5), 58 (1990).

³C.H. Brito Cruz, R.L. Fork, W.H. Knox, and C.V. Shank, *Chem. Phys. Lett.* **132**, 341 (1986).

⁴R.L. Schoemaker and F.A. Hopf, *Phys. Rev. Lett.* **33**, 1527 (1974).

⁵M.S. Rosker, F.W. Wise, and C.L. Tang, *Phys. Rev. Lett.* **57**, 321 (1986).

⁶M. Mitsunaga and C.L. Tang, *Phys. Rev. A* **35**, 1720 (1987).

⁷Y.R. Shen, *The Principles of Nonlinear Optics* (Wiley and Sons, New York, 1984).

⁸K. Duppen, F. Haan, E.T.J. Nibbering, and D.A. Wiersma, *Phys. Rev. A* **47**, 5120 (1992).

⁹I.D. Abella, N.A. Kurmit, and S.R. Harman, *Phys. Rev.* **141**, 3911 (1966).

¹⁰W.H. Hesselink and D.A. Wiersma, *J. Chem. Phys.* **73**, 648 (1980).

¹¹I.S. Osad'ko and M.V. Stashek, *Zh. Eksp. Teor. Fiz.* **106**, 535 (1994) [*JETP* **79**, 293 (1994)].

¹²C.H. Brito Cruz, J.P. Gordon, P.C. Becker, R.L. Fork, and C.V. Shank, *J. Quantum Electron.* **24**, 261 (1988).

¹³T.A. Pham, A. Daunois, J.C. Merle, J. Le Moigne, and J.Y. Bigot, *Phys. Rev. Lett.* **74**, 904 (1995).

¹⁴M. Aihara, *Phys. Rev. B* **21**, 2051 (1980).

¹⁵Y. Kayanuma, *Phys. Rev. B* **41**, 3360 (1990).

¹⁶S. Saikan, J.W.I. Lin, and H. Nemoto, *Phys. Rev. B* **46**, 11 125 (1992).

¹⁷S. Saikan, J.W.I. Lin, and H. Nemoto, *Phys. Rev. B* **46**, 7123 (1992).

¹⁸Y.J. Yan and S. Mukamel, *J. Chem. Phys.* **94**, 179 (1990).

- ¹⁹R. Kubo, *J. Math. Phys.* **4**, 174 (1963).
- ²⁰Erik T.J. Nibbering, Douwe A. Wiersma, and Koos Duppen, *Phys. Rev. Lett.* **66**, 2464 (1991).
- ²¹J.-Y. Bigot, M.T. Portella, R.W. Schoenlein, C.J. Bardeen, A. Migus, and C.V. Shank, *Phys. Rev. Lett.* **66**, 1138 (1991).
- ²²R.F. Loring and S. Mukamel, *Chem. Phys. Lett.* **114**, 426 (1985).
- ²³B.D. Fainberg, *Opt. Spectrosc. (USSR)* **55**(6), 669 (1983).
- ²⁴J.L. Skinner and D. Hsu, *J. Phys. Chem.* **90**, 4931 (1986).
- ²⁵M. Aihara, *Phys. Rev. B* **25**, 53 (1982).
- ²⁶M. Aihara and M. Hama, *Phys. Rev. B* **52**, 3366 (1995).
- ²⁷I.S. Osad'ko, *J. Luminesc.* **56**, 197 (1993).
- ²⁸Y. Kayanuma, *J. Phys. Soc. Jpn.* **57**, 292 (1987).
- ²⁹V. Hizhnyakov and I. Tehver, *Phys. Status Solidi* **21**, 755 (1967).
- ³⁰S. Mukamel, *J. Chem. Phys.* **73**, 5322 (1980).
- ³¹T. Takagahara, E. Hanamura, and R. Kubo, *J. Phys. Soc. Jpn.* **44**, 728 (1978).
- ³²I.S. Osad'ko and S.N. Gladenkova, *Chem. Phys. Lett.* **198**, 531 (1992).
- ³³J.P. Lavoine, A.J. Boeglin, P. Martin, and A.A. Villaeys, *Phys. Rev. B* **53**, 11 535 (1996).
- ³⁴T. Yajima and Y. Taira, *J. Phys. Soc. Jpn.* **47**, 1620 (1979).